JOURNAL OF MATERIALS RESEARCH AND TECHNOLOGY 2023;26:99–108

Available online at www.sciencedirect.com

jmr&t Journal of Materials Research and Technology

journal homepage: www.elsevier.com/locate/jmrt

Review Article

# Sustainable substrate tin oxide/nanofibril cellulose/thermoplastic starch: dimensional stability and tensile properties

*N.A. Azra Master Degree, Student* [a],
*A. Atiqah Ph.D, Senior Lecturer, Research Fellow* [a,*],
*A. Jalar Ph.D, Professor, Principal Research Fellow* [a,b],
*G. Manar Ph.D, Senior Lecturer, Research Fellow* [c,g,h,i,**],
*A.B.M. Supian Ph.D, Research Fellow* [d,e],
*R.A. Ilyas Ph.D, Senior Lecturer, Research Fellow* [f,g,h,i]

[a] *Institute of Microengineering and Nanoelectronics, Universiti Kebangsaan Malaysia, Bangi, Selangor, 43600 UKM, Malaysia*
[b] *Department of Applied Physics, Faculty of Science and Technology, Universiti Kebangsaan Malaysia, Bangi, Selangor, 43600 UKM, Malaysia*
[c] *Department of Aeronautical Engineering and Aviation, Faculty of Engineering, National Defence University of Malaysia, Kem Perdana Sungai Besi, 57000 Kuala Lumpur, Malaysia*
[d] *Centre for Defence Research and Technology (CODRAT), Universiti Pertahanan National Malaysia, Kem Perdana Sungai Besi, 57000 Kuala Lumpur, Malaysia*
[e] *Institute of Energy Infrastructure, Universiti Tenaga Nasional, Jalan IKRAM-UNITEN, Kajang, 43000 Selangor, Malaysia*
[f] *Institute of Tropical Forest and Forest Products (INTROP), Universiti Putra Malaysia, Serdang, 43400 UPM, Selangor, Malaysia*
[g] *Centre for Advanced Composite Materials, Universiti Teknologi Malaysia, Johor Bahru, 81310 Johor, Malaysia*
[h] *Faculty of Chemical and Energy Engineering, Universiti Teknologi Malaysia, Iskandar Puteri, 81310 UTM, Johor, Malaysia*
[i] *Centre of Excellence for Biomass Utilization, Universiti Malaysia Perlis, Arau, 02600 Perlis, Malaysia*

ARTICLE INFO

*Article history:*
Received 15 April 2023
Accepted 10 July 2023
Available online 20 July 2023

*Keywords:*
Sustainable substrate

ABSTRACT

Polymers used in thin films or substrates contribute to several environmental issues hence biodegradable materials should be used instead. In order to overcome this issue, the use of sustainable filler and reinforcements are needed to replace the existing synthetic materials. Nevertheless, the lower mechanical properties and higher water absorption could be hindered by incorporating Tin oxide (SnO) in nanofibril cellulose reinforced thermoplastic starch (NCF/TPS). In this study, different content of SnO (0, 1, 2, 3, 4, and 5 wt.%) with NCF/TPS nanocomposites was prepared by stir casting methods. The characterisation in terms

* Corresponding author. Institute of Microengineering and Nanoelectronics, Universiti Kebangsaan Malaysia, Bangi, 43600 UKM, Selangor, Malaysia.
** Corresponding author. Department of Aeronautical Engineering and Aviation, Faculty of Engineering, National Defence University of Malaysia, Kem Perdana Sungai Besi, 57000 Kuala Lumpur, Malaysia.
E-mail addresses: nikathirahazzra2@gmail.com (N.A. Azra), a.atiqah@ukm.edu.my (A. Atiqah), azmn@ukm.edu.my (A. Jalar), gunasilan@upnm.edu.my (G. Manar), mohdsupian7779@gmail.com (A.B.M. Supian).
https://doi.org/10.1016/j.jmrt.2023.07.088

Thermoplastic starch/nanofibril
Cellulose/TinOxide
Dimensional stability
Tensile properties

of dimensional stability (density, water absorption, and thickness swelling) and tensile properties were studied. From the finding, it was found that the highest content of SnO leads to the lowest density, water absorption, and thickness swelling properties of SnO/NCF/TPS blend nanocomposites. Moreover, the incorporation of SnO at 4 wt.% shows good tensile properties than other formulations of SnO/NCF/TPS.



## 1. Introduction

In these last few years, polymer-based material can be found everywhere in our daily life. The use of polymer-based wearable sensors is capable to monitor our health in a real-time system [1,2]. The over-produced non-biodegradable polymer like polypropylene (PP), low-density polyethylene, and polyether ether ketone (PEEK) have drawn a critical environmental issue also resulting in ecological imbalance [3–6]. In order to overcome this issue, academia has taken the initiative in fabricating biopolymers to replace synthetic polymer-based materials [7]. Biopolymer here refers to bio-based material which come from natural resources like starch [8–15], chitosan [16–18], polylactic acid (PLA) [19–22], and cellulose [21,23–25].

There has been a lot of study work on using thermoplastic starch as a strain sensor [26–29], starch/Polydimethylsiloxane (PDMS) to monitor aquatic-product freshness monitoring [26], and thermoplastic starch/graphite for electrochemical catechol sensor [30]. The use of starch-based polymer materials have good electrical properties, though the lower mechanical properties can be enhanced by incorporating metallic nanoparticles and nanocellulose. The metallic nanofiber to strengthen the TPS nanocomposites can be found with the incorporation of silver nanoparticle (AgNP)/sugar palm starch reported by Rozilah et al. [31], the addition of AgNPs in the composite improved the tensile strength by 165 kPa for every 1 wt.% of AgNPs. However, excessive AgNPs loading leads to stiffer films and reduces mechanical properties. Similar findings by Knitter et al. [32] on fabricating biodegradable composite of Mater-Bi modified with silver, composite with the highest Ag content leads to the lower impact strength.

Another study done by Mohanty et al. [33] investigated nano-bio composites of nano-silver embedded in starch/poly (ethymethacrylate) (PEMA), the tensile results showed increases as the AgNP were added from 0.0 wt.% to 2.0 wt.%, there are significant increases in the tensile strength from approximately 62.3 MPa to ~72.0 MPa. This tensile strength is related to the density of the composites. In another work, Syafiq et al. [34] studied the effect of cinnamon essential oil (CEO) when added to nanocellulose fibre–reinforced starch biopolymer composites. The results show that as the content of CEO added increased, the tensile strength improved from 4.8 to 5.3 MPa. In terms of dimensional stability properties, the density of the composites decreased from 1.38 to 1.31 g/cm$^3$ affecting the composite to be stiffer and not flexible. Water absorption test was also conducted to check on the water uptake rate, the percentage of water absorption decreases as the CEO content increases, which improve waterproof properties. This water barrier test is crucial to examine the physical properties of the composites. Gürler and Torgut et al. [35] have improved the mechanical, barrier and electrical properties of graphene-reinforced potato starch composite films. They obtained a comparable result that adding graphene to the films also increases the tensile strength. Thickness swelling test was carried out to analyse the water barrier properties, since graphene is hydrophobic, adding it would shift the natural potato starch behaviour to become more resistant towards water.

The use of tin oxide (SnO) with NCF/TPS nanocomposites is novel to this study. SnO is a semiconducting substance that is often used in a variety of applications. It has a band gap of around 3.6 eV, showing its usefulness as a semiconductor [36]. The band gap is the difference in energy between the valence and conduction bands, which determines the electrical properties of a material. Moreover, SnO has distinctive properties due to its broad band gap. The band gap is the difference in energy between the valence and conduction bands, which determines the electrical properties of a material. It can function as a conductive material when appropriately doped or under specific conditions. This makes it valuable for electrical conductivity applications like electronic devices and sensors. Furthermore, SnO is compatible and readily integrated into starch-based products with thermoplastic starch. This permits the development of conductive materials with improved properties. As a natural, biodegradable, and renewable polymer, starch contributes sustainability to the composite [2,7,37]. The use of SnO may also be deposited as a thin film on various substrates, such as starch-based films or coatings. This promotes the incorporation of SnO into flexible or complicated structures, making it suited for use in flexible electronics and biodegradable sensors.

To the best of our knowledge, there are no works concerning SnO/NCF/TPS nanocomposites, despite the ease of production of sugar palm NCF and their reinforcing effect when mixed with the TPS matrix [38]. SnO was chosen as the conductive filler, it may not be as conductive as silver [39], gold [40] or copper [41], but the conductivity is adequate for the research. Moreover, according to Environmental Protection Agency (EPA) with CAS Reg. No. 18282-10-5 under FFDCA section 408(d) [42], SnO is not harmful towards humans and the environment. However, it is not safe to be inhaled directly as it will disrupt the respiratory system. This study used powdered SnO to fabricate thin films with a low percentage amount. Thus, it is safe to use SnO for the conducting materials for this study. Considering the material's cost, SnO are economically and environmentally safe to use. Therefore, the present work aims at studying the effect of SnO reinforced with NCF on TPS nanocomposites. The composition was prepared by stir casting at 95 wt.% TPS, SnO and NCF ranged from

0 to 5 wt.% regarding the TPS phase. The physical, tensile, and morphological properties were investigated.

## 2. Experimental

### 2.1. *Materials*

The raw material fabricating this substrate was nanofiber cellulose (NCF) suspension from Oil Palm Empty Fruit Bunches (OPEFB) obtained from ZoepNano Sdn. Bhd., Serdang, Selangor, Malaysia. Meanwhile, thermoplastic starch sugar palm in powder form was purchased from PT Kofta Unitrada, Tangerang, Indonesia. Stannous Oxide/Tin (II) Oxide (SnO) brand Aldrich was purchased from Evergreen Engineering Resources Sdn. Bhd., Semenyih, Selangor, Malaysia in micron particle size (≤60) and 97% powder.

### 2.2. *Preparation of SnO/NCF/TPS nanocomposites*

SnO/NCF/TPS samples were prepared using the stir casting method by referring to Ilyas et al. [43] with some improvements to the existing method. The details improvement in pre-preparations was needed, whereby 1% NCF and 4% SnO were weighed and sonicated for 30 min in 180 ml distilled water to ensure both NCF and SnO were dispersed well. In the following method, approximately 7 g of TPS with a 1:1 ratio of glycerol and sorbitol was added and heated over the hot plate with a magnetic stirrer for 10 min at 85 °C and a speed of 1000 rpm. Then, 150 ml of the suspension was poured into a 20 cm × 8 cm mould (see Table 1).

**Table 1 – Composition of SnO/NCF/TPS nanocomposites.**

| Sample | SnO (wt.%) | NCF (wt.%) | TPS (wt.%) |
|---|---|---|---|
| 0SnO/5NCF/TPS | 0 | 5 | 95 |
| 1SnO/4NCF/TPS | 1 | 4 | 95 |
| 2SnO/3NCF/TPS | 2 | 3 | 95 |
| 3SnO/2NCF/TPS | 3 | 2 | 95 |
| 4SnO/1NCF/TPS | 4 | 1 | 95 |
| 5SnO/0NCF/TPS | 5 | 0 | 95 |

## 3. Characterization

### 3.1. *Density*

The density of the substrate was determined through the ASTM D4018 standards test, where all six samples were immersed in distilled water to weigh in both dry and wet mass of the sample using a Mettler Toledo XS205 electronic densitometer. The final density of the substrate was obtained through the density formula in equation (1):

$$\text{Density}, \rho = \frac{m}{V} \quad (1)$$

where $\rho$, = Density (g/cm$^3$), m = Mass (g), $\upsilon$ = Average volume (cm$^3$)

### 3.2. *Water absorption & thickness swelling*

The substrate's water absorption rate was conducted according to ASTM D570-98. All the initial weights of the samples were marked as 0 h. For the next 24 h, samples were removed from distilled water and marked as final weight as in 24 h. Data were taken continuously up till 216 h. Lastly, all the data were analysed through the following equation (2) to finalise the water absorption rate.

$$\text{Water absorption } (\%) = \frac{W_f - W_i}{W_i} \text{ x } 100 \quad (2)$$

where, $W_f$ = Final weight and $W_i$ = Initial weight of substrate.

### 3.3. *Thickness swelling*

The substrate's thickness swelling rate was conducted similarly to the water absorption test, which was also following ASTM D 570 standards. The initial thickness of the sample was measured using a vernier calliper and recorded as 0 h, then continued immersed in the distilled water. After 24 h, data was marked as 24 h until 216 h. Equation (3) below was used to calculate the fraction of thickness swelling.

$$\text{Thickness swelling } (\%) = \frac{T_f - T_i}{T_i} \text{ x } 100 \quad (3)$$

where $T_f$ = Final thickness and $T_i$ = Initial thickness of substrate.

### 3.4. *Tensile testing*

The tensile specimen was conditioned at 37 °C for 48 ± 2 h prior to testing. The specimens were individually fixed in a vice that grips onto a universal testing machine with a load cell of 5 kN and a crosshead speed of 50 mm/min. The failure load was recorded in newtons (N). The value of the tensile strength was calculated using the following Equation (4):

$$TS = F/A \quad (4)$$

where TS is the tensile strength (N/mm$^2$), F is the load at failure (N), and A is the area of a cross-section at failure (mm$^2$).

### 3.5. *Surface morphology*

For sample preparation of SnO/NCF/TPS, the surfaces of six specimens were coated with gold to avoid electrostatic charging at the surface of the specimen. Using a MERLIN, ZEISS Field emission scanning electron microscope (FE-SEM), the SnO/NCF/TPS's surface morphology was evaluated. Images obtained from FESEM were captured at a voltage of 3 kV and magnification of 2.00 k X equipped with an energy-dispersive X-ray analysis (EDX). A sample of 5 mm in height was cut from the composite and used for morphology analysis.

### 3.6. *Statistical analysis*

Statistical analyses of the data were performed using the using one-way analysis of variance (ANOVA) with the aid of

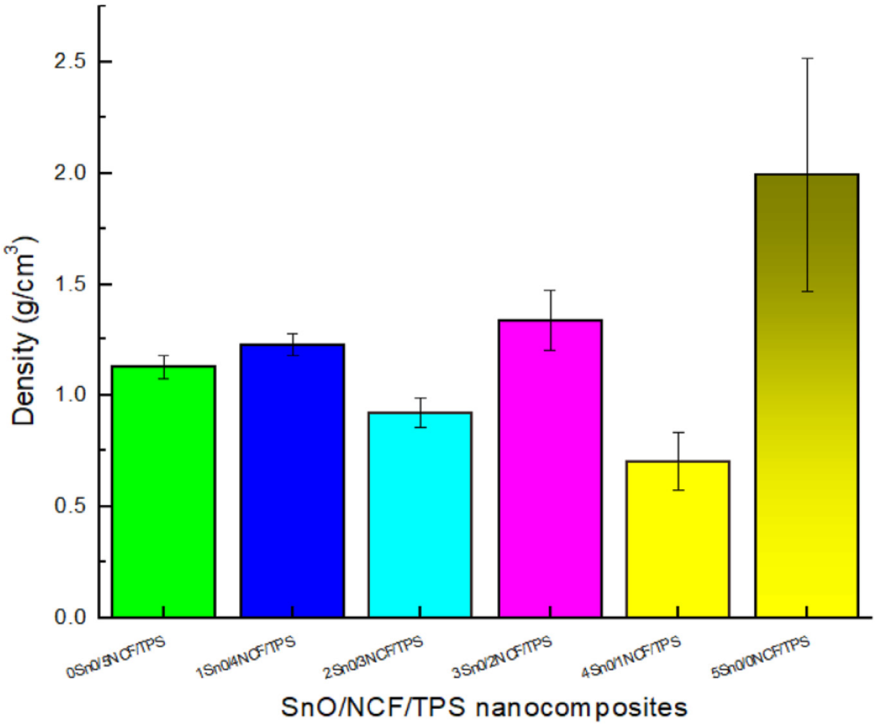


**Fig. 1 – Density properties of SnO/NCF/TPS nanocomposites.**

the Data Analysis ToolPak in Microsoft Excel to determine the significance level (5%) of the effect of the composition of SnO wt.% (from 0 until 5 wt.%). The measured data for the density and tensile properties were statistically compared using one-way analysis of variance. The significance level was set at $p \leq 0.05$.

## 4. Results and discussion

### 4.1. *Density*

Density is the most crucial part of sample characterization as it correlates to the other testing like tensile, water absorption,

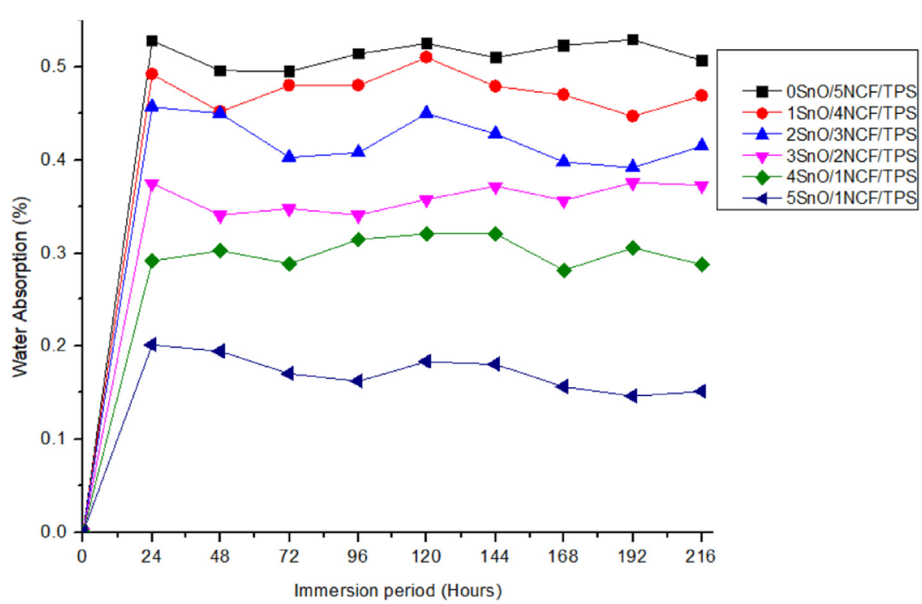


**Fig. 2 – Water absorption of SnO/NCF/TPS nanocomposites.**

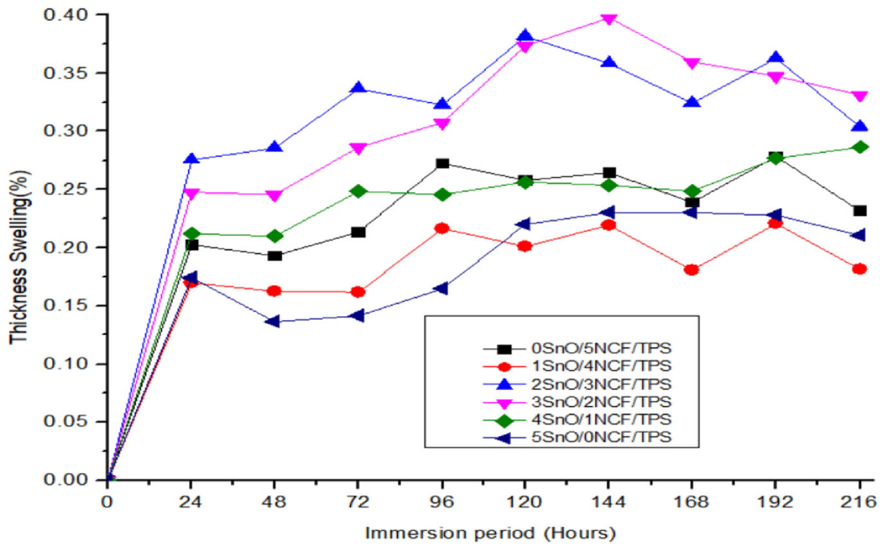


**Fig. 3 – Thickness swelling of SnO/NCF/TPS nanocomposites.**

thickness swelling and even in surface morphology. Fig. 1 presented density for six different compositions of SnO/NCF/TPS substrate. As expected, the substrate with the highest content of SnO (5SnO/0NCF/TPS) achieved the highest density, 1.3889 g/cm$^3$.According to the raw data for density, SnO has the highest density of 6.45 g/cm$^3$ [44] followed by TPS with 1.54 g/cm$^3$ [45], then NCF marked the lowest density of 1.15 g/cm$^3$ [46]. The study is aligned with our previous finding that the high-density composite comes from low NCF content [47]. Therefore, the addition of conductive filler SnO will also increase the density of the matrix.

### 4.2. *Water absorption*

The prepared substrate contains nanofibril cellulose mainly from empty oil palm fruit bunch. Consequently, it was expected the physical properties would be highly able to engage with water as it has high hydrophilic properties or, by other means, a shallow resistant act towards water. However, in the presence of tin oxide, there are changes in the amount of water uptake since it was highly repulsive towards water (hydrophobic properties). Fig. 2 depicts the outcomes from the water absorption test conducted for at least 10 days, approximately 216 h. For the first 24 h, all six substrates recorded a sharp increase in the amount of water uptake led by substrate 0SnO/5NCF/TPS containing 5% NCF without any additional SnO. Meanwhile, substate 5SnO/0NCF/TPS marked the lowest. The best explanation that fits in the data observed is that substrate with high NCF content tends to absorb more water than substrate with high SnO. This is correlated to the fact that NCF has a high affinity towards water compared to SnO. Another issue that may influence the amount of water uptakes is the availability of void, fibre content and density of the composite [48,49]. According to Radzi et al. [50], increasing weight of the composite is due to the water trapped inside void that formed in between the composite structure. By taking account of that, this explains sample 5SnO/0NCF/TPS has fewer voids since it contains SnO with a larger diameter,

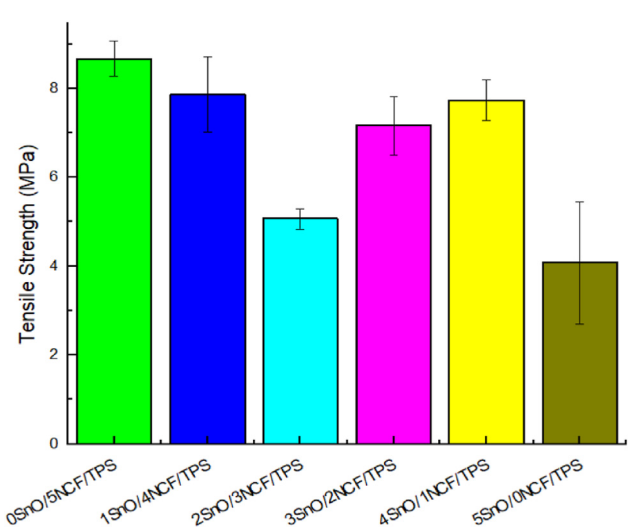


**Fig. 4 – Tensile strength of SnO/NCF/TPS nanocomposites.**

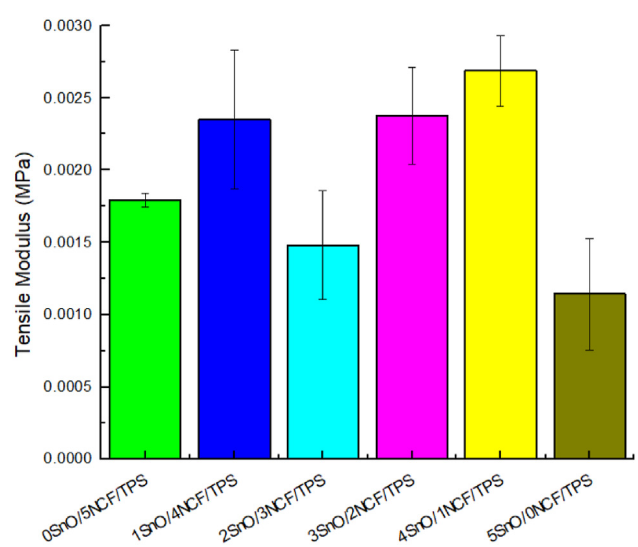


**Fig. 5 – Tensile Modulus properties of SnO/TPS nanocomposites.**

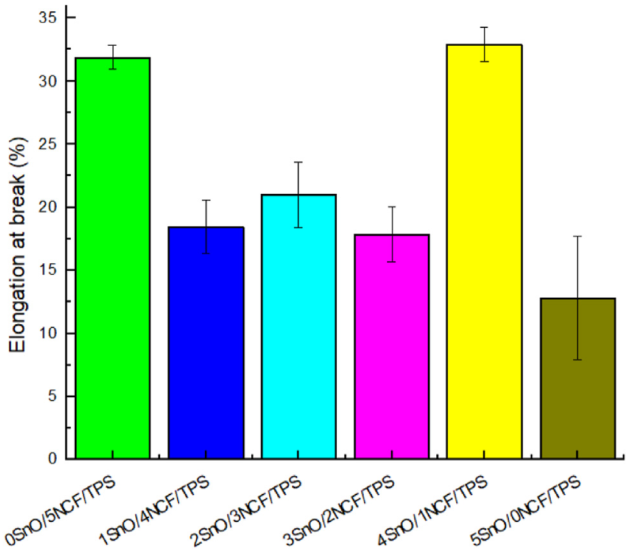


**Fig. 6 – Elongation of break SnO/NCF/TPS nanocomposites.**

higher density and even greater water resistance than NCF. After 24 h, all substrates remain almost consistent for another few days indicating they have reached the maximum volume of water absorbed at the equilibrium state [51].

### 4.3. *Thickness swelling*

As shown in Fig. 3, SnO/NCF/TPS nanocomposites exhibited less thickness swelling when immersed in distilled water more than 120 h. At 0 until 144 h, the highest thickness swelling was subjected to 1SnO/4NCF/TPS followed by 5SnO/0NCF/TPS, 0SnO/1NCF/TPS, 1SnO/4NCF/TPS, 2SnO/3NCF/TPS and 3SnO/2NCF/TPS. The highest range of thickness swelling was 0.40% after 216 h showing that the nanocomposites were resistance to swelling conditions. The least thickness swelling value at 216 h was subjected to 1SnO/4NCF/TPS and exhibited less hydrophilic behaviours with a better rigid structure. Even though the value of thickness swelling of higher content does not show less thickness swelling, and this can be inferred that the cumulative pore volume that existed in nanocomposites was closely aligned. The sturdy hydrogen-bonded nanocellulose structure of the fibre ensured that the building elements remained firm and tightly bound. This resulted in the formation of negligible interfacial voids [52]. In most cases, the hydrophilic property of natural fibre is the determining factor in water absorption. It affects the thickness as well as the swelling. An improvement in nanocomposites dimensional stability was seen when SnO was incorporated. The reduction in water uptake yielded better interfacial bonding and higher resistance to water absorption.

### 4.4. *Tensile test*

Regarding the tensile strength of SnO/NCF/TPS nanocomposites, depicted in Fig. 4, the trend when incorporating SnO filler concentration in NCF/TPS nanocomposites. The highest tensile strength was subjected to 0SnO/5NCF/TPS followed by 1SnO/4NCF/TPS, 3SnO/2NCF/TPS, 4SnO/1NCF/TPS, 2SnO/3NCF/TPS and 5SnO/0NCF/TPS. There is decrement by 9% at 1 wt.% SnO filler concentration, when compared to 0SnO/5NCF/TPS specimens. The major reason for the increase of tensile strength of 0SnO/5NCF/TPS was likely to be the consequence of the strong interactions between NCF and TPS. These interactions allowed load transfer from NCF to starch, subsequently enhancing the reinforcing ability [53]. In similar research regarding the incorporation of oil empty fruit bunch filler concentration with cassava starch [38], the value of tensile strength ranged between 0.5 and 3 MPa lowered than our finding with the incorporation of NCF (4–8.8 MPa) were improved due to the nanofibril size distribution homogenous will be discussed in Section 4.6. Another research by reported similar values but with less improvement in the tensile strength (0–400 kPa) regarding the incorporation of silver nanoparticles (0–4 wt.% AgNPs) with sugar palm thermoplastic starch due to the agglomeration of the particles led to the weak interaction of the AgNPs on SPS/TPS nanocomposites [31].

Moreover, the tensile modulus as depicted in Fig. 5 increases for concentrations up to 4 wt.% of SnO and rapidly decreases in higher concentrations at 5 wt.% SnO, as shown in Fig. 5, is the highest value in the case of 4SnO/1NCF/TPS. Since the nanoparticles agglomerate, several factors might contribute to an increase in the material's strength, including their interaction with the polymer matrix. When determining the material properties of the finished composite, the adequate size of the filler plays a significant impact. A basic rule states that the effective filler surface area will grow alongside the interactions with the matrix in proportion to the reduction in the size of the filler particles. In addition, when there is a more significant concentration of filler, the polymer chains are immobilised, and there is a considerable concentration of stress at the locations of agglomeration [4]. This leads to the formation of fracture sites, reducing the composite's overall mechanical properties. The fact that the tensile strength and the tensile modulus of elasticity of the nanocomposites tested in this study increased (up to specific concentrations for each nanomaterial, as indicated) is evidence that the circumstance indicated above is accurate.

The elongation of SnO reinforced NCF/TPS nanocomposite films is shown in Fig. 6. There is a gradual reduction in the elongation at the break of the nanocomposites with the increasing of various proportions of SnO, except for 4 wt.% SnO. Similar patterns in the elongation at break with increasing CNC of the nanocomposite films were also discovered for PVA/gelatin films containing water hyacinth cellulose nanocrystals. This may be because the incorporation of CNC results in the formation of three-dimensional network structures inside the nanocomposite films, contributing to an increase in the films' stiffness [15]. It was also discovered that incorporating nanocellulose into alginate-based films led to a decrease in the films' elongation after being broken [30].

However, a further drop in SnO/NCF/TPS loading resulted in a decrease in the elongation at break, except at 4 wt.% SnO, which might impact the flexibility of SnO/NCF/TPS nanocomposite films. This might be explained by the fact that the excessive addition of SnO constrained the molecular chain of starch. Specifically for the sample that included 5 wt.% SnO, the elongation at break was only 57.38%, which resulted in an

**Table 2 – Statistical analysis for properties of SnO/NCF/TPU nanocomposites.**

Anova: Single Factor

SUMMARY

| *Groups* | *Count* | *Sum* | *Average* | *Variance* |
|---|---|---|---|---|
| Density (g/cm$^3$) | 6 | 7.308839 | 1.21814 | 0.194625 |
| Tensile Strength (MPa) | 6 | 40.57499 | 6.762498 | 3.212999 |
| Tensile Modulus (MPa) | 6 | 0.011832 | 0.001972 | 3.57E-07 |
| Elongation (%) | 6 | 134.7948 | 22.46579 | 66.42701 |

ANOVA

| *Source of Variation* | SS | *df* | MS | F | *P-value* | *F crit* |
|---|---|---|---|---|---|---|
| Between Groups | 1920.905 | 3 | 640.3016 | 36.67531 | 2.54E-08 | 3.098391 |
| Within Groups | 349.1732 | 20 | 17.45866 | | | |
| Total | 2270.078 | 23 | | | | |

easily broken substrate. The sample that included 4 wt.% of SnO had a good elongation at break and a noticeable rise in tensile modulus and tensile strength, as seen in Figs. 4 and 5. The incorporation of the 4% SnO (4SnO/1NCF/TPS) could be the highest strength due to the higher content of 4% SnO, this is probably the good distribution of 4% SnO with NCF/TPU as compared to 0SnO/5NCF/TPS and 5SnO/0NCF/TPS. With the proper combination of 4% SnO and 1% NCF is improved the highest tensile properties. While for 0SnO/5NCF/TPS, the sample only have 5 wt% of NCF with no SnO. Moreover, the tensile properties do not achieving higher when the higher content of SnO and NCF. We could suggest that with the hybridization of metallic inorganic particles and nanofibril cellulose could enhance the properties of nanocomposites. Therefore, the inclusion of NCF into TPS nanocomposite films at 5 wt.% could significantly strengthen the tensile strength compared to other contents of SnO and NCF (see Table 1).

### 4.5. *Statistical analysis*

The effect of composition on the physical and tensile properties of SnO/NCF/TPU nanocomposites. The four variations of density, tensile strength, tensile modulus and elongation properties were analyzed using analysis of variance (ANOVA) of the mechanical properties Single factor to determine the significance of the composition SnO/NCF/TPU nanocomposites. From Table 2, P-value showed less than 0.05 ($P < 0.05$), which shows the composition led to different properties of SnO/NCF/TPU nanocomposites since the P-value is below 0.05 ($p < 0.05$), a statistically significant difference the

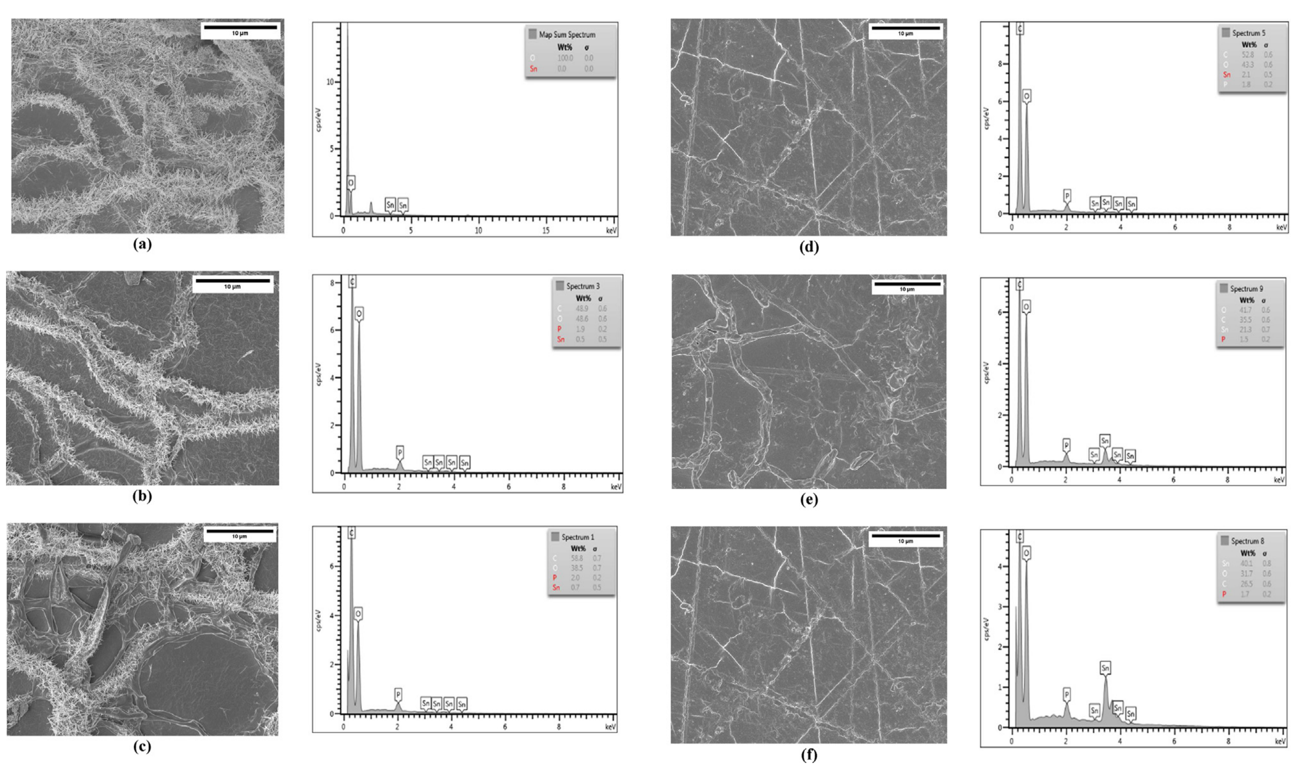


**Fig. 7 – FESEM morphology and EDX spectrum of (a) 0SnO/5NCF/TPS, (b) 1SnO/4NCF/TPS, (c) 2SnO/3NCF/TPS, (d) 3SnO/2NCF/TPS, (e) 4SnO/1NCF/TPS, and (f) 5SnO/0NCF/TPS.**

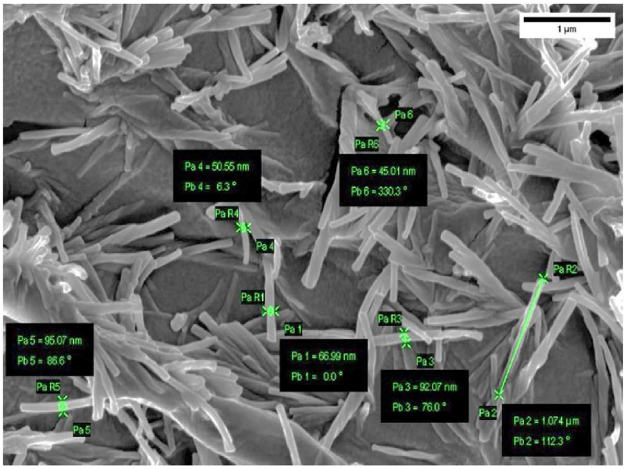


**Fig. 8 – FESEM morphology of Nanocellulose-fibril with range of diameter.**

Sn composition towards the mean of density, tensile strength, tensile modulus and elongation properties to another.

### 4.6. *Surface morphology*

FESEM is a surface imaging tool capable of obtaining resolutions at diverse particle sizes, size distributions, nanomaterial forms, and surface morphologies of produced particles at the micro and nanoscale. To determine the properties of SnO and NCF films and optimize their performance, it was necessary to understand the sizes, shapes, and surfaces of the aggregation states of SnO/NCF/TPS films. Incorporating SnO, a more significant percentage but smaller in size, proved beneficial in strengthening the molecular bonding on the films. Incorporating SnO had a greater percentage but was smaller in size proved beneficial in terms of strengthening the molecular bonding on the films. FESEM inspection of the surfaces was conducted so that the dispersion of SnO and NCF in TPS could be better understood. The FESEM morphology along with EDX images of 6 specimens of 0SnO/5NCF/TPS, 1SnO/4NCF/TPS, 2SnO/3NCF/TPS, 3SnO/2NCF/TPS, 4SnO/1NCF/TPS, and 5SnO/0NCF/TPS were shown in Fig. 7 (a)-(f). The EDX spectrum indicates the percentage of SnO was increased accordingly to the addition of SnO to the substrate. Fig. 7 (a) portrayed a disordered lamellar structure with an aggregating bulk component. This is due to the higher content of 5 wt.% NCF leads the agglomeration of NFC in TPS. The increase of SnO from Fig. 7 (b) until (f) showed aggregations became smaller and less aligned to a smooth surface, as shown in Fig. 7 (e), indicating better dispersion of 4 wt.% SnO in TPS matrix. This could be attributed to the particles of SnO, and NCF can promote the interaction between filler and the hydrophilic matrix. The EDX quantitative and qualitative analysis confirmed that the SnO in NCF/TPS nanocomposites films contained SnO, and the content was 0, 0.5%, 0.7%, 2.1%, 21.3% and 26.5% respectively (Fig. 7 (a)–(f)). On the other hand, Fig. 8 shows a closer look on 0SnO/5NCF/TPS under 20.00 K X magnification to observe the diameter of NCF. The NCF are in the network of fibre form diameters ranging between 45.01 nm and 95.07 nm.

## 5. Conclusion

The functional interaction in the films that included SnO had a favourable effect on the physical and tensile properties, both of which are essential for the performance of sustainable substrate applications. In addition, the results of the physical properties indicated that the density properties of SnO/NCF/TPS nanocomposites do not shift despite an increase in the amount of SnO and NCF. SnO was successfully incorporated into NCF/TPS nanocomposite films, providing films with the potential for conducting film. The results of this study showed that good compatibility between NCF/TPS and SnO. There was an increment in tensile strength and tensile modulus values on the NCF/TPS films incorporated with SnO, ranging from 4.1 to 8.7 MPa and 23.5–42.9 MPa respectively. The density and moisture content values decreased respectively with increasing SnO concentration. The results indicated that 4 wt.% SnO contents significantly affected tensile strength, tensile modulus, elongation at break, tensile strain, density, water absorption and thickness swelling properties. Overall, it can be deduced that the developed films incorporated with SnO could be considered a potential alternative for sustainable films in term of physical and tensile properties.

## Declaration of Competing Interests

The authors declare the following financial interests/personal relationships which may be considered as potential competing interests: A. Atiqah reports financial support was provided by National University of Malaysia Institute of Microengineering and Nanoelectronics. A. Atiqah reports a relationship with National University of Malaysia Institute of Microengineering and Nanoelectronics that includes: employment.

## Acknowledgement

The authors would like to thank the Graduate Research Assistantship (GRA) programme support by Universiti Kebangsaan Malaysia under grant GUP-2022-072 of the Ministry of Higher Education Malaysia and Universiti Pertahanan Nasional Malaysia (UPNM) under grant UPNM/2022/GPJP/TK/6 for laboratory work and publication funding.

## REFERENCES

[1] Harito C, Utari L, Putra BR, Yuliarto B, Purwanto S, Zaidi SZJ, et al. Review—the development of wearable polymer-based sensors: perspectives. J Electrochem Soc 2020;167:037566. https://doi.org/10.1149/1945-7111/ab697c.

[2] Kheirabadi S, Sheikhi A. Recent advances and challenges in recycling and reusing biomedical materials. Curr Opin Green Sustain Chem 2022:100695.

[3] Das PP, Chaudhary V. Materials Today : proceedings Environmental impact and effect of chemical treatment on

bio fiber based polymer composites. Mater Today Proc 2021. https://doi.org/10.1016/j.matpr.2021.03.097.
[4] Ilyas RA, Sapuan SM, Ishak MR, Zainudin ES, Atikah MSN. Characterization of sugar palm nanocellulose and its potential for reinforcement with a starch-based composite. In: Sugar palm biofibers, biopolym. Biocomposites. 1st ed., ed. Boca Raton, FL: CRC Press/Taylor & Francis Group; 2018. p. 189–220. https://doi.org/10.1201/9780429443923-10. CRC Press.
[5] Daud MY, Aziz A. Bamboo-fiber-reinforced thermoset and thermoplastic potential applications. 2022.
[6] Ilyas RA, Sapuan SM, Atiqah A, Asyraf MRM, Nurazzi NM, Norrrahim MNF, et al. Thermal properties of sugar palm fiber-based hybrid composites. Nat Fiber-Reinforced Compos Therm Prop Appl 2022:53–83.
[7] Jiang D-H, Ree BJ, Isono T, Xia X-C, Hsu L-C, Kobayashi S, et al. Facile one-pot synthesis of rod-coil bio-block copolymers and uncovering their role in forming the efficient stretchable touch-responsive light emitting diodes. Chem Eng J 2021;418:129421.
[8] Syafri E, Yulianti E, Asrofi M, Abral H, Sapuan SM, Ilyas RA, et al. Effect of sonication time on the thermal stability, moisture absorption, and biodegradation of water hyacinth (Eichhornia crassipes) nanocellulose-filled bengkuang (Pachyrhizus erosus) starch biocomposites. J Mater Res Technol 2019;8:6223–31.
[9] Ilyas RA, Sapuan SM, Nazrin A, Syafiq R, Aisyah HA, Norrrahim MNF, et al. Nanocellulose/starch biopolymer nanocomposites: processing, manufacturing, and applications. Elsevier Inc.; 2020. https://doi.org/10.1016/B978-0-12-819661-8.00006-8.
[10] Ilyas RA, Sapuan SM, Ishak MR, Zainudin ES. Development and characterization of sugar palm nanocrystalline cellulose reinforced sugar palm starch bionanocomposites. Carbohydr Polym 2018;202:186–202. https://doi.org/10.1016/j.carbpol.2018.09.002.
[11] Syafiq RMO, Ilyas RA, Rajeshkumar L, AL-Oqla FM, Nukman Y, Zuhri MYM, et al. Corn starch nanocomposite films reinforced with nanocellulose. 2023. https://doi.org/10.1515/psr-2022-0011.
[12] Ilyas RA, Azmi A, Nurazzi NM, Atiqah A, Atikah MSN, Ibrahim R, et al. Oxygen permeability properties of nanocellulose reinforced biopolymer nanocomposites. Mater Today Proc 2022;52:2414–9.
[13] Ilyas RA, Asyraf MRM, Aisyah HA, Sapuan SM, Norrrahim MNF, Ibrahim R, et al. Introduction to nanocellulose production from biological waste. In: Ind. Appl. Nanocellulose its nanocomposites. Elsevier; 2022. p. 1–37.
[14] Mukaffa H, Asrofi M, Hermawan Y, Qoryah RDH, Sapuan SM, Ilyas RA, et al. Effect of alkali treatment of piper betle fiber on tensile properties as biocomposite based polylactic acid: solvent cast-film method. Mater Today Proc 2022;48:761–5.
[15] Ilyas RA, Sapuan SM, Ibrahim R, Abral H, Ishak MR, Zainudin ES, et al. Thermal, biodegradability and water barrier properties of bio-nanocomposites based on plasticised sugar palm starch and nanofibrillated celluloses from sugar palm fibres. J Biobased Mater Bioenergy 2020;14:234–48. https://doi.org/10.1166/jbmb.2020.1951.
[16] Jiménez-Gómez CP, Cecilia JA. Chitosan: a natural biopolymer with a wide and varied range of applications. Molecules 2020;25. https://doi.org/10.3390/molecules25173981.
[17] Gaabour LH. Influence of silica nanoparticles incorporated with chitosan/polyacrylamide polymer nanocomposites. J Mater Res Technol 2019;8:2157–63.
[18] Menazea AA, Ismail AM, Awwad NS, Ibrahium HA. Physical characterization and antibacterial activity of PVA/Chitosan matrix doped by selenium nanoparticles prepared via one-pot laser ablation route. J Mater Res Technol 2020;9:9598–606.
[19] Ruz-Cruz MA, Herrera-Franco PJ, Flores-Johnson EA, Moreno-Chulim MV, Galera-Manzano LM, Valadez-González A. Thermal and mechanical properties of PLA-based multiscale cellulosic biocomposites. J Mater Res Technol 2022;18:485–95.
[20] Liu Z, Lei Q, Xing S. Mechanical characteristics of wood, ceramic, metal and carbon fiber-based PLA composites fabricated by FDM. J Mater Res Technol 2019;8:3741–51.
[21] Lu W, Cui R, Zhu B, Qin Y, Cheng G, Li L, et al. Influence of clove essential oil immobilized in mesoporous silica nanoparticles on the functional properties of poly (lactic acid) biocomposite food packaging film. J Mater Res Technol 2021;11:1152–61.
[22] Sreekumar K, Bindhu B, Veluraja K. Perspectives of polylactic acid from structure to applications. Polym Renew Resour 2021;12:60–74. https://doi.org/10.1177/20412479211008773.
[23] Shahdan D, Chen RS, Ahmad S. Optimization of graphene nanoplatelets dispersion and nano-filler loading in bio-based polymer nanocomposites based on tensile and thermogravimetry analysis. J Mater Res Technol 2021;15:1284–99.
[24] Atiqah A, Ansari MNM, Kamal MSS, Jalar A, Afeefah NN, Ismail N. Effect of alumina trihydrate as additive on the mechanical properties of kenaf/polyester composite for plastic encapsulated electronic packaging application. J Mater Res Technol 2020;9:12899–906.
[25] Shaghaleh H, Xu X, Wang S. Current progress in production of biopolymeric materials based on cellulose, cellulose nanofibers, and cellulose derivatives. RSC Adv 2018;8:825–42. https://doi.org/10.1039/c7ra11157f.
[26] Wang F, Qiu L, Tian Y. Super anti-wetting colorimetric starch-based film modified with poly (dimethylsiloxane) and micro-/nano-starch for aquatic-product freshness monitoring. Biomacromolecules 2021;22:3769–79.
[27] Huang B, Zhu L, Wei S, Li Y, Nie Y, Zhao W. Starch-based ion-conductive organo-hydrogels with self-healing, anti-freezing, and high mechanical properties towards strain sensors. Macromol Rapid Commun 2023:2200890.
[28] He L, Ye D, Weng S, Jiang X. A high-strength, environmentally stable, self-healable, and recyclable starch/PVA organohydrogel for strain sensor. Eur Polym J 2022;181:111650.
[29] Si W, Weng Y, Tan B, Zhang S. Adopted ion-pair effect to construct bicontinuous starch-based gel and its application in humidity sensitivity and strain-responsiveness. Compos B Eng 2022;234:109696.
[30] de Freitas A de SM, Maciel CC, Lemes AP, Ferreira M. Thermoplastic starch and graphite biocomposite electrode for electrochemical catechol sensor. ECS Adv 2022;1:36504.
[31] Rozilah A, Jaafar CNA, Sapuan SM, Zainol I, Ilyas RA. The effects of silver nanoparticles compositions on the mechanical, physiochemical, antibacterial, and morphology properties of sugar palm starch biocomposites for antibacterial coating. Polymers 2020;12:2605.
[32] Knitter M, Czarnecka-komorowska D. Manufacturing and Properties of Biodegradable Composites Based on Thermoplastic Starch/Polyethylene-Vinyl Alcohol and Silver Particles n.d.;4:610–624. https://doi.org/10.1007/978-3-030-16943-5.
[33] Mohanty F, Swain SK. Nano silver embedded starch hybrid graphene oxide sandwiched poly(ethylmethacrylate) for packaging application. Nano-Structures and Nano-Objects 2019;18:100300. https://doi.org/10.1016/j.nanoso.2019.100300.
[34] Syafiq R, Sapuan SM, Zuhri MRM. Antimicrobial activity, physical, mechanical and barrier properties of sugar palm

based nanocellulose/starch biocomposite films incorporated with cinnamon essential oil. J Mater Res Technol 2021;11:144–57.
[35] Gürler N, Torğut G. Graphene-reinforced potato starch composite films: improvement of mechanical, barrier and electrical properties. Polym Compos 2021;42:173–80. https://doi.org/10.1002/pc.25816.
[36] Cai X, Zhang P, Wei S-H. Revisit of the band gaps of rutile SnO2 and TiO2: a first-principles study. J Semiconduct 2019;40:92101.
[37] Azad MM, Ejaz M, Afaq SK, Song J. A bio-based approach to simultaneously improve flame retardancy, thermal stability and mechanical properties of nano-silica filled jute/thermoplastic starch composite. Mater Chem Phys 2022;289:126485.
[38] Perera UP, Foo ML, Chew IML. Effect of nanolignin and nanocrystalline cellulose on thermal, mechanical, and water barrier properties of starch composites. In: Sustain. Technol. Oil palm ind. Latest adv. Case Stud. Springer; 2022. p. 117–37.
[39] Du X, Zhang Z, Liu W, Deng Y. Nanocellulose-based conductive materials and their emerging applications in energy devices - a review. Nano Energy 2017;35:299–320. https://doi.org/10.1016/j.nanoen.2017.04.001.
[40] Tommalieh MJ, Awwad NS, Ibrahium HA, Menazea AA. Characterization and electrical enhancement of PVP/PVA matrix doped by gold nanoparticles prepared by laser ablation. Radiat Phys Chem 2021;179:109195. https://doi.org/10.1016/j.radphyschem.2020.109195.
[41] Hashim A, Habeeb MA, Hadi A. Synthesis of novel polyvinyl alcohol–starch-copper oxide nanocomposites for humidity sensors applications with different temperatures. Sens Lett 2017;15:1–4. https://doi.org/10.1166/sl.2017.3876.
[42] Able T. 55970 dates, vol. 83. AGENCY; 2018. p. 55970–4.
[43] Ilyas RA, Sapuan SM, Atiqah A, Ibrahim R, Abral H, Ishak MR, et al. Sugar palm (Arenga pinnata [Wurmb.] Merr) starch films containing sugar palm nanofibrillated cellulose as reinforcement: water barrier properties. Polym Compos 2020;41:459–67. https://doi.org/10.1002/pc.25379.
[44] Pfaff G, Bonnet JP. Influence of SnO on the sintering behaviour of tin dioxide. Ceram Int 1997;23:257–61. https://doi.org/10.1016/S0272-8842(96)00036-3.
[45] Atikah MSN, Ilyas RA, Sapuan SM, Ishak MR, Zainudin ES, Ibrahim R, et al. Degradation and physical properties of sugar palm starch/sugar palm nanofibrillated cellulose bionanocomposite. Polimery 2019;64:680–9. https://doi.org/10.14314/polimery.2019.10.5.
[46] Zuhri M, Yusoff M, Mohd Sapuan S, Ismail N, Wirawan R. Mechanical properties of short random oil palm fibre reinforced epoxy composites. Sains Malays 2010;39:87–92.
[47] Azra NA, Atiqah A, Fadhlina H, Bakar MA, Jalar A, Ilyas RA, et al. Oil-palm based nanocellulose reinforced thermoplastic polyurethane for plastic encapsulation of biomedical sensor devices: water absorption, thickness swelling and density properties. Appl Sci Eng Prog 2022. https://doi.org/10.14416/j.asep.2022.02.001.
[48] Vilay V, Mariatti M, Mat Taib R, Todo M. Effect of fiber surface treatment and fiber loading on the properties of bagasse fiber–reinforced unsaturated polyester composites. Compos Sci Technol 2008;68:631–8. https://doi.org/10.1016/j.compscitech.2007.10.005.
[49] Nunna S, Chandra PR, Shrivastava S, Jalan AK. A review on mechanical behavior of natural fiber based hybrid composites. J Reinforc Plast Compos 2012;31:759–69.
[50] Radzi AM, Sapuan SM, Jawaid M, Mansor MR. Water absorption, thickness swelling and thermal properties of roselle/sugar palm fibre reinforced thermoplastic polyurethane hybrid composites. J Mater Res Technol 2019;8:3988–94. https://doi.org/10.1016/j.jmrt.2019.07.007.
[51] Yorseng K, Rangappa SM, Pulikkalparambil H, Siengchin S, Parameswaranpillai J. Accelerated weathering studies of kenaf/sisal fiber fabric reinforced fully biobased hybrid bioepoxy composites for semi-structural applications: morphology, thermo-mechanical, water absorption behavior and surface hydrophobicity. Construct Build Mater 2020;235:117464. https://doi.org/10.1016/j.conbuildmat.2019.117464.
[52] Nazrin A, Sapuan SM, Zuhri MYM. Mechanical, physical and thermal properties of sugar palm nanocellulose reinforced thermoplastic starch (Tps)/poly (lactic acid) (pla) blend bionanocomposites. Polymers 2020;12:1–18. https://doi.org/10.3390/polym12102216.
[53] Orue A, Eceiza A, Arbelaiz A. Preparation and characterization of poly (lactic acid) plasticized with vegetable oils and reinforced with sisal fibers. Ind Prod 2018;112:170–80.

**Nik Athirah Azzra Nik Badrul Ehsan**: is a Postgraduate Student at Institute of Microengineering and Nanoelectronics, Universiti Kebangsaan Malaysia, Malaysia.

**Dr. Atiqah Mohd Afdzaluddin**: is a Senior Lecturer/Research Fellow at Institute of Microengineering and Nanoelectronics, Universiti Kebangsaan Malaysia, Malaysia.

**Prof. Dr. Azman Jalar**: is a Professor at Department of Applied Physics, Faculty of Science and Technology, and Institute of Microengineering and Nanoelectronics, Universiti Kebangsaan Malaysia, Malaysia.

**Dr. Gunasilan Manar**: is Senior Lecturer at Department of Aeronautical Engineering and Aviation, Faculty of Engineering, National Defence University of Malaysia

**Dr. Mohd Supian Abu Bakar**: is External Research Fellow, Centre of Defense Research and Technology, Universiti Pertahanan Nasional Malaysia.

**Dr. Ahmad Ilyas Rushdan**: is a Senior Lecturer in Faculty of Chemical and Energy Engineering, Universiti Teknologi Malaysia, 81310 UTM, Iskandar Puteri, Johor, Malaysia